

Discrete averaging for maps

A. Vieiro

Universitat de Barcelona

Joint work with V. Gelfreich (U. Warwick)

Recent Advances in Dynamical Systems, Oviedo, 1-5 junio 2026

Motivational framework: beam dynamics in plasma physics

The analysis of accelerator-beam dynamics is an important topic in plasma physics. This is usually modelled by a (close-to-)symplectic return map.

In this setting, averaging for near-identity maps and the corresponding adiabatic invariants are used to control particle trapping into resonances.

Adiabatic trapping:

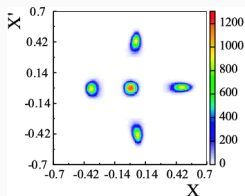
- Simplifies modeling: manageable equations to design of plasma devices.
- Explains confinement: when fields **change slowly**, adiabatic invariants let you predict how particles move and whether they stay trapped or escape.
- **Evolution wrt parameters** of adiabatic invariants is useful to **split a particle beam into separate beams**.

Drawbacks:

- Physics: Requires slow field variation; imperfect adiabaticity causes scattering or partial trapping; collisions and nonideal fields reduce effectiveness.
- Mathematics: Iterates can be experimentally recorded but the actual expression of the return map is approximated; the computation of the adiabatic invariant involves a transformation to a normal form.

Beam dynamics, the Hénon map and the adiabatic invariant

The conservative Hénon map is the simplest standard model. Particular interest: the bifurcation near the 1:4 resonance (degenerate).



2D beam distribution of the split beam in the transfer line downstream of the Proton-Synchrotron extraction point (Gilardoni et al. Phys.Rev.ST 9, 2006).

Previous works: Adiabatic invariant obtained via transformation to a higher-order normal form.

Alternative? We will show that **discrete averaging** allows one to determine the adiabatic invariant **directly in the original coordinates**, without recourse to normal form transformations, and to carry out a systematic analysis of the domain of validity of the adiabatic approximation.

Applications of discrete averaging go far beyond the context of this example.

Classical averaging theory – overview

The averaging theory studies systems that can be written in the form

$$\dot{x} = a(x, \varphi), \quad \varepsilon \dot{\varphi} = b(x, \varphi),$$

where a and b are periodic in φ with a period $T > 0$. If $|b| \geq c > 0$, the implicit function theorem allows to reduce the study to a non-autonomous equation of the form

$$x' = \varepsilon f(x, \tau),$$

with a non-autonomous time-periodic vector field f .

Averaged system: The solution of the (autonomous) averaged system

$$y' = \varepsilon \bar{f}(y), \quad \text{where} \quad \bar{f}(y) = \frac{1}{T} \int_0^T f(y, \tau) d\tau,$$

gives the leading order approximation for trajectories starting from a point x_0 at $\tau = 0$: if $x(0, x_0) = y(0, x_0) = x_0$ then

$$x(\tau, x_0) = y(\tau, x_0) + O(\varepsilon) \quad \text{for } |\tau| \leq C/\varepsilon, \quad C > 0.$$

Classical averaging theory – adiabatic invariants

The integrals of motion of the averaged equation play the role of adiabatic invariants for the original system as they change slowly in time.

Higher order adiabatic theory: a close to the identity time-periodic change of coordinates, $z = u_n(x, \tau)$, can be used to eliminate the time-dependence in the leading orders:

$$z' = \varepsilon f_n(z, \varepsilon) + \varepsilon^{n+1} g(z, \tau, \varepsilon).$$

Well-known property. An integral h_n of the truncated system $z' = \varepsilon f_n(z, \varepsilon)$ evaluated on a trajectory of the original system oscillates with an amplitude $O(\varepsilon)$ but stays near its initial value for substantially longer times $O(\varepsilon^{-n})$.

Relation with near-id maps: If $(x(t), \varphi(t))$ is a solution of $\dot{x} = a(x, \varphi), \varepsilon \dot{\varphi} = b(x, \varphi)$, there is an increasing sequence t_k that corresponds to consecutive intersections of the solution with the Poincaré section $\{\varphi = 0 \pmod{T}\}$. Then $x_k = x(t_k)$ is a trajectory of the first return map $F_\varepsilon : x_k \mapsto x_{k+1}$. Since the return time is small, the first return map is close to the identity, $F_\varepsilon = \text{id} + O(\varepsilon)$.

Problem: Following this suspension+averaging approach, computing h_n is hard.

Discrete averaging – interpolating vector fields (IVFs)

Discrete averaging provides explicit expressions for autonomous IVFs $X_{n,\varepsilon}$ such that

$$F_\varepsilon = \Phi_{X_{n,\varepsilon}}^1 + O(\varepsilon^{n+1}).$$

in terms of weighted averages over a trajectory segment. Then the adiabatic invariants can be obtained from the IVFs $X_{n,\varepsilon}$.

Interpolating vector fields. Let n_0 and n be two integers with $0 \leq n_0 \leq n$. The integer n defines the length of a trajectory segment and n_0 is used to select a starting point. There is a unique polynomial $P_n(t, x)$ of degree n in t which interpolates a segment of the orbit of a point x :

$$P_n(k, x) = F^k(x) \quad \text{for } k = -n_0, \dots, n - n_0.$$

The IVF is defined as the derivative of $P_n(t, x)$ at $t = 0$:

$$X_n(x) = \frac{\partial P_n}{\partial t}(0, x).$$

IVFs are explicit and computationally inexpensive

$X_n(x)$ is a weighted sum of the iterates of $F(x)$: the Lagrange interpolation procedure gives

$$P_n(t, x) = \sum_{k=-n_0}^{n-n_0} b_k(t) F^k(x), \quad \text{where} \quad b_k(t) = \prod_{\substack{-n_0 \leq j \leq n-n_0 \\ j \neq k}} \frac{t-j}{k-j}.$$

Consequently,

$$X_n(x) = \sum_{k=-n_0}^{n-n_0} p_{nk} F^k(x),$$

where the coefficients $p_{nk} = b'_k(0)$ depend on n and n_0 but are **independent of the map F** . For example, for $(n_0, n) = (0, 1)$ and $(1, 2)$ we get respectively

$$X_1(x) = F(x) - x, \quad \text{and} \quad X_2(x) = \frac{1}{2}(F(x) - F^{-1}(x)).$$

Application: The Hénon map 1:4 resonance

The Hénon map $H_c : (x, y) \mapsto (c(1 - (x + 1)^2) + 2x + y, -x)$ has two fixed points $p_e = (0, 0)$ and $p_h = (-2, 2)$. When $c = 1$, p_e is at the 1:4 resonance.

Not generic: for $c = 1 + \varepsilon$ with $\varepsilon > 0$ there is a 4-periodic hyperbolic orbit at a distance $\mathcal{O}(\sqrt{\varepsilon})$ from p_e whose invariant manifolds form a chain of four islands of stability containing a 4-periodic elliptic orbit at a distance $\mathcal{O}(\sqrt[4]{\varepsilon})$ from p_e . We use **discrete averaging** to study the bifurcation:

The central interpolation scheme applied to $F_\varepsilon = H_{1+\varepsilon}^4$ provides the IVF

$X_2(x, y, \varepsilon) = \frac{1}{2} (H_{1+\varepsilon}^4(x, y) - H_{1+\varepsilon}^{-4}(x, y))$, such that

$$H_{1+\varepsilon}^4 - \Phi_{X_2}^1 = \mathcal{O}_9(x, y) + \varepsilon \mathcal{O}_7(x, y) + \mathcal{O}(\varepsilon^2).$$

We use integration to extract the Hamiltonian part of the vector field X_2 . If

$$h_2(x, y, \varepsilon) = \int_0^1 X_2(tx, ty) \cdot (y, -x) dt,$$

then

$$X_2(x, y, \varepsilon) - \left(\frac{\partial h_2}{\partial y}, -\frac{\partial h_2}{\partial x} \right) (x, y, \varepsilon) = \mathcal{O}_8(x, y) + \varepsilon \mathcal{O}_5(x, y) + \mathcal{O}(\varepsilon^2).$$

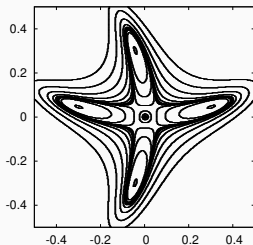
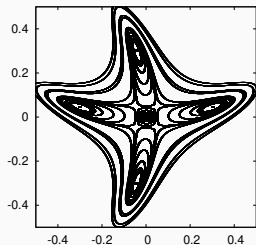
Moreover, one can check that h_2 is an adiabatic invariant **of** $H_{1+\varepsilon}$ such that

$$h_2 \circ H_{1+\varepsilon}(x, y, \varepsilon) - h_2(x, y, \varepsilon) = \mathcal{O}_9(x, y) + \varepsilon \mathcal{O}_7(x, y) + \mathcal{O}(\varepsilon^2).$$

Application: The Hénon map 1:4 resonance – adiabatic invariant

One has $h_2 = \tilde{h}_2 + \mathcal{O}((x+y)^7, \varepsilon^2)$, with

$$\begin{aligned}\tilde{h}_2 = & -x^2y^2 + x^4y - xy^4 - \frac{x^6}{3} + 2x^3y^3 - \frac{y^6}{3} + x^2y^5 - x^5y^2 \\ & + \varepsilon \left(2(x^2 + y^2) + 2xy(y - x) + (x^2 - y^2)^2 + 3x^4y - 2x^3y^2 + 2x^2y^3 - 3xy^4 \right. \\ & \left. + \frac{1}{3}(-4x^6 + 6x^5y - 17x^4y^2 + 24x^3y^3 - 17x^2y^4 + 6xy^5 - 4y^6) \right)\end{aligned}$$



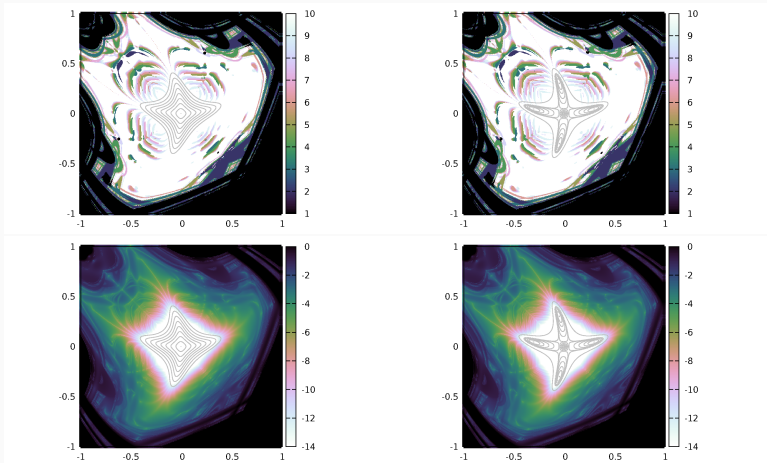
Iterates of the Hénon map (left) and level lines of h_2 (right) for $c = 1 + \varepsilon$, $\varepsilon = 10^{-3}$.

- Computations were done directly **in original coordinates**.
- A higher accuracy approximation can be achieved using X_n , $n > 2$.
- No need of algebraic manipulators to numerically evaluate X_n or h_n .

Application: The Hénon map 1:4 resonance – bifurcation

Q: Where can the discrete averaging be used to analyze the dynamics?

For a mesh of points $(x, y) \in [-1, 1]^2$, we compute the integer n minimizing $G_{(x,y)}(n) = |X_{2n}(x, y) - X_{2n+2}(x, y)|_2$. **Plot:** We display n and $\log_{10} G_{(x,y)}(n)$.



IVF theory: $G_{(x,y)}(n) = \mathcal{O}(\epsilon^{2n+1})$ where $\epsilon =$ distance of the map to the identity.

IVF theory - approximation by autonomous flow

Let $D \subset \mathbb{R}^d$ be an open domain and consider a smooth family of maps $F_\varepsilon : D \rightarrow \mathbb{R}^d$ that is *tangent to identity*, i.e.,

$$F_\varepsilon(x) = x + \varepsilon f(x, \varepsilon), \quad f(x, \varepsilon) = \sum_{k=0}^{n-1} \varepsilon^k f_k(x) + \varepsilon^n r_n(x, \varepsilon), \quad r_n \text{ bounded.}$$

Theorem 1. If a tangent to identity family $F_\varepsilon \in \mathcal{C}^{n+1}(D \times [-\varepsilon_0, \varepsilon_0])$ for some $\varepsilon_0 > 0$, then there is a unique polynomial in ε vector field

$g(x, \varepsilon) = \sum_{k=0}^{n-1} \varepsilon^k g_k(x)$ such that

$$F_\varepsilon = \Phi_{\varepsilon g_\varepsilon}^1 + O(\varepsilon^{n+1})$$

uniformly on every compact subset of D . Moreover, for $1 \leq k \leq m \leq n$

$$\frac{1}{k!} \left. \frac{\partial^k X_m}{\partial \varepsilon^k} \right|_{\varepsilon=0} = g_{k-1},$$

where X_m is an interpolating vector field of order m and consequently

$$F_\varepsilon = \Phi_{X_m}^1 + O(\varepsilon^{m+1}).$$

Comment: The error decays faster for larger m but there is no information on the constant in the O -term. Therefore it is not possible to use this theorem to decide what order of interpolation leads to the most accurate approximation for a fixed value of ε .

IVF theory - uniform bounds

Let $\epsilon, \delta > 0$. For a set $D_0 \subset \mathbb{C}^d$, let D_δ be a δ -neighbourhood of D_0 . We denote by $\mathcal{C}^\omega(D_\delta, \mathbb{C}^d)$ the space of all analytic maps $F : D_\delta \rightarrow \mathbb{C}^d$ equipped with the supremum norm $\|\cdot\|_{D_\delta}$. Let $B_\epsilon(D_\delta) \subset \mathcal{C}^\omega(D_\delta, \mathbb{C}^d)$ be the closed ball of radius ϵ centered at the identity map: an analytic map $F \in B_\epsilon(D_\delta)$ iff

$$\|F - \text{id}\|_{D_\delta} \leq \epsilon.$$

Let $M_\alpha = \lfloor c_0/\alpha \rfloor + 1$ where $c_0 = 1/(6e) = 0.061\dots$

Theorem 2. Let $\epsilon, \delta > 0$ be such that $\epsilon/\delta \leq c_0$ and $D_0 \subset \mathbb{C}^d$. Then for any map $F \in B_\epsilon(D_\delta)$ the IVF of order $m \in [2, M_{\epsilon/\delta}]$ satisfies $\|X_m\|_{D_{\delta/3}} \leq 2\epsilon$ and

$$\|\Phi_{X_m}^1 - F\|_{D_0} \leq 3\epsilon \left(\frac{6(m-1)\epsilon}{\delta} \right)^m.$$

In particular, for $m = M_{\epsilon/\delta}$, one has $\|\Phi_{X_m}^1 - F\|_{D_0} \leq 3\epsilon \exp(-c_0 \delta/\epsilon)$.

Comments.

- Useful for **individual maps** (not necessarily embedded in a near-identity family).
- The error is controlled by the ratio ϵ/δ where δ characterizes the size of the complex neighbourhood where the map is ϵ -close to the identity.

Sketch of the proof of Theorem 2.

We consider

$$f_\mu = (1 - \mu) \text{id} + \mu F, \quad \mu \in \mathbb{C}.$$

One has

$$X_m(x) = \sum_{k=1}^m \frac{(-1)^{k-1}}{k} \Delta_k(x),$$

$$\Delta_0(x) = x, \quad \Delta_k(x) = \Delta_{k-1}(F(x)) - \Delta_{k-1}(x), \quad k \geq 1.$$

1. Limit flow. For $|\mu| \leq \mu_1 = \delta/\epsilon$,

$$\|X_{1,\mu}\|_{D_\delta} = \|f_\mu - \text{id}\| = \|\mu(F - \text{id})\|_{D_\delta} \leq |\mu|\epsilon \leq \delta$$

$$\implies \|\Phi_{X_{1,\mu}}^1 - f_\mu\|_{D_0} \leq \|\Phi_{X_{1,\mu}}^1 - \text{id}\|_{D_0} + \|\text{id} - f_\mu\|_{D_0} \leq 2|\mu|\epsilon.$$

Then, the MMP on the disk $|\mu| \leq \mu_1$ implies that $\|\Phi_{X_1}^1 - F\|_{D_0} \leq 2\epsilon^2/\delta$.

2. Bounds for the finite differences in $D_{\delta/3}$. Let $m \geq 2$ and $\mu_m = \frac{2\delta}{3\epsilon(m-1)}$.

$$\Delta_m(x_0) = \sum_{k=0}^{m-1} (-1)^{m-k-1} \binom{m-1}{k} \Delta_1(x_k) \implies \|\Delta_m\|_{D_{\delta/3}} \leq 2^{m-1} |\mu| \epsilon.$$

Then, the MMP on $\mu \leq \mu_m$ implies $\|\Delta_m\|_{D_{\delta/3}} \leq 2^{m-1} \mu_m \epsilon (|\mu|/\mu_m)^m$.

Maximum modulus principle (MMP): If g analytic in the open disk $|\mu| < r$ and $g^{(k)}(0) = 0$, $0 \leq k < m$, then $|g(\mu)| \leq (|\mu|/r)^m \sup_{|\mu| < r} |g(\mu)|$.

Sketch of the proof of Theorem 2.

3. Bounds for $\|X_{m,\mu}\|_{D_{\delta/3}}$ with $2 \leq m \leq M_{\epsilon/\delta}$. For $|\mu| \leq \mu_m/4$,

$$\|X_{m,\mu}\|_{D_{\delta/3}} \leq \sum_{k=1}^m \frac{\|\Delta_k\|_{D_{\delta/3}}}{k} \leq \epsilon \sum_{k=1}^m \frac{2^{k-1}|\mu|^k}{k\mu_k^{k-1}} \leq \epsilon \sum_{k=1}^m \frac{2^{k-1}|\mu|^k}{\mu_m^{k-1}} \leq 2\epsilon|\mu|.$$

Since $\mu_m > 4$ for $2 \leq m \leq M_{\epsilon/\delta}$ we can substitute $\mu = 1$ and get

$$\|X_m\|_{D_{\delta/3}} \leq 2\epsilon.$$

4. Approximation of F by the time-one map of X_m in D_0 . It follows that $\|\Phi_{X_{m,\mu}}^1 - f_\mu\|_{D_0} \leq \|\Phi_{X_{m,\mu}}^1 - \text{id}\|_{D_0} + \|\text{id} - f_\mu\|_{D_0} \leq 3\epsilon|\mu|$.

Then, the MMP on $|\mu| \leq \mu_m/4$ implies

$$\|\Phi_{X_m}^1 - F\|_{D_0} \leq 3\epsilon \left(\frac{4}{\mu_m}\right)^m = 3\epsilon \left(\frac{6\epsilon(m-1)}{\delta}\right)^m.$$

For $m = M_{\epsilon/\delta}$ we obtain the exponentially small upper bound.

Dynamics near a resonant equilibrium - hidden symmetries of IVFs

If $f(0) = 0$ is fully resonant (i.e. the Jacobian is a root of unity), there is $n \geq 1$ s.t. f^n is **tangent to identity**: $(f^n)'(0) = (f'(0))^n = Id$.

Then, there is a unique formal vector field X such that the **formal series** for the time- n flow defined by X coincide with f^n , i.e. $\Phi_X^n = f^n$.

If f is symplectic, then X is Hamiltonian and $h_X \circ f^n = h_X \circ \Phi_X^n = h_X$.

Lemma. Let f be a formal diffeomorphism with $f(0) = 0$ such that f^n is tangent to the identity for some $n \in \mathbb{N}$, and let X be the formal vector field such that $f^n = \Phi_X^n$. Then the vector field X is **f -invariant**, i.e.,

$$X \circ f = D(f)X, \quad \text{where } D(f) \text{ is the Jacobian matrix.}$$

Moreover, if f is symplectic, then X is Hamiltonian with a formal Hamiltonian h_X and

$$h_X \circ f = h_X.$$

Comment: This was observed for the Hénon map:

the IVF computed for H_c^4 gives an adiabatic invariant for H_c .

On the interpolation scheme to compute IVFs

Any interpolation scheme can be used to compute IVFs but...

The **Newton forward interpolation scheme** is a convenient tool for **analytical proofs** as it avoids inversion of the original map.

For example, we used it to **proof the optimal Nekhoroshev estimates** for a family of real-analytic symplectic maps of the form

$$F_\varepsilon : \begin{cases} \bar{I} = I + \varepsilon a(I, \varphi), \\ \bar{\varphi} = \varphi + \omega(I) + \varepsilon b(I, \varphi) \pmod{1}, \end{cases}$$

depending on $\varepsilon \geq 0$, $I \in \mathbb{R}^d$, a, b are periodic in $\varphi \in \mathbb{T}^d = \mathbb{R}^d / \mathbb{Z}^d$, under the assumption that $\omega = h'_0$ with h_0 strongly convex:

Nekhoroshev estimates. There are $c_1, c_2, c_3 > 0$ such that for every initial condition (I_0, φ_0) one has

$$|I_k - I_0| < c_1 \varepsilon^{1/2(d+1)} \quad \text{for} \quad 0 \leq k \leq T_\varepsilon = c_2 \exp\left(c_3 \varepsilon^{-1/2(d+1)}\right).$$

Nekhoroshev theorem - where IVFs are used?

Our “Lochak-Neishtadt” direct proof of the exponentially long stability times relies on the following observations.

- We construct a **covering of the action space** by open neighbourhoods of a finite number (depending on ϵ) of unperturbed tori bearing periodic motions (maximum resonances).
- For every $n \ll \epsilon^{-1/2}$, the covering identifies domains where F_ϵ^n is close to the identity. Each of these domains is centered at $I = I_*$ such that $n\omega(I_*) \in \mathbb{Z}^d$, corresponding to a torus invariant by F_0 foliated by invariant n -periodic orbits.
- In these domains, **we use IVFs** to show that F_ϵ^n is exponentially close to the **time-one map of an autonomous Hamiltonian flow**.

Since the Hamiltonian flow preserves its Hamiltonian function H_n , we conclude that $H_n \circ F_\epsilon^n - H_n$ is exponentially small.

- The leading order approximation for H_n can be obtained from analysis of the integrable map F_0^n . The **convexity assumption** can be used to show that there is a small neighbourhood of $I = I_*$ which can be represented as a union of level sets of H_n . For an initial condition that is not too close to its boundary, an exponentially large number of iterates of F_ϵ^n is needed to achieve a change in H_n sufficiently large to leave the neighbourhood.

In practice, use any interpolation scheme to compute IVFs but...

The [Stirling-Newton central interpolation scheme](#) is often a better tool for numerical simulations as it provides more accurate approximations. For example, we used it for [visualization of 4D near-id dynamics](#).

“Poincaré” sections: Let $\Sigma = \{x \in \mathbb{R}^m : g(x) = 0\}$ be a smooth codim-1 hyper-surface. Take x_0 and iterate $x_{k+1} = f_\epsilon(x_k)$. If $g(x_k)g(x_{k+1}) \leq 0$ and X_1 is (locally) transversal to Σ then, for ϵ small enough, $\exists!$ $t_k \in [0, \epsilon]$ s.t.

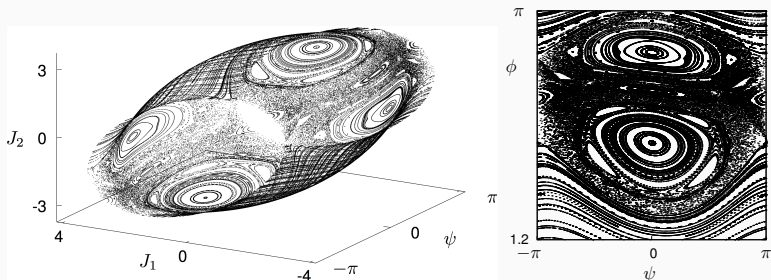
$$g(\Phi_{X_n}^{t_k}(x_k)) = 0.$$

→ Plot $y_k = \Phi_{X_n}^{t_k}(x_k)$ instead of (any other projection of) x_k .

Visualizing the dynamics of 4D near-id symplectic maps

Example (Froeschlé-like map). We consider the 4D map T_ε of $\mathbb{T}^2 \times \mathbb{R}^2$ given by $(\psi, J) \mapsto (\bar{\psi}, \bar{J}) = (\psi_1 + \varepsilon(\bar{J}_1 + a_2 \bar{J}_2), \psi_2 + \varepsilon(a_2 \bar{J}_1 + a_3 \bar{J}_2), J_1 - \varepsilon \sin \psi_1, J_2 - \varepsilon \delta \sin \psi_2)$ and $\Sigma = \{\psi_1 = \psi_2\}$. On a moderate time scale, the iterates of x_0 remain close to the “energy surface” $\{x : h_n(x) = h_n(x_0)\}$.

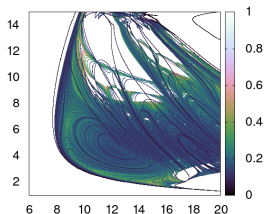
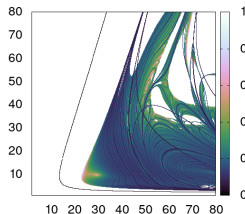
Plot: $T_{0.35}$, 400 i.c. on $\Sigma \cap \{h_{10} = 4\}$, 500 iterates



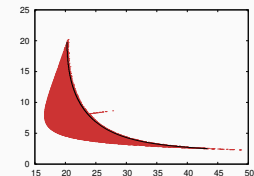
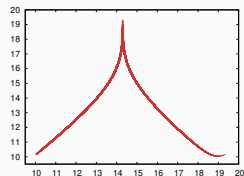
Comment: Allows to rigorously explore Arnold diffusion both qualitative and quantitative (with error estimates). It works better closer to double resonances!

Other settings to use IVFs: Discrete Lorenz attractors

Lorenz map: $\bar{x} = x + \delta(\sigma(y - x))$, $\bar{y} = y + \delta(\bar{x}(\rho - z) - y)$, $\bar{z} = z + \delta(\bar{x}y - 8z/3)$.



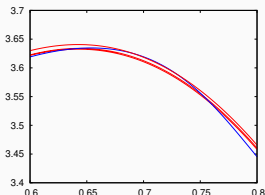
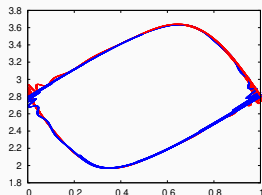
For δ small, we use IVFs to compute kneading diagram, (ρ, σ) -parameter space (top right $\delta = 0.001$, top left $\delta = 0.06$), reduce dynamics to 1D-“Poincaré maps” (bottom left, $\delta = 0.001$), and determine the region with pseudohyperbolic discrete Lorenz-like attractors (bottom right, $\delta = 0.01$).



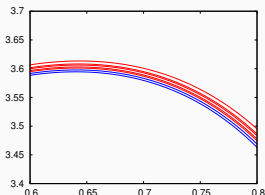
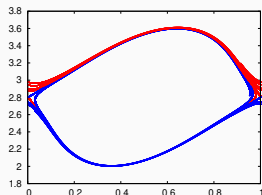
To do: Use IVFs to convert numerical evidence into a direct proof for the existence of discrete Lorenz attractors.

Other settings to use IVFs: probability of capture (weak dissipation)

Dissipative standard map (top) vs IVF (bottom)



Transversal
intersection
of $W^{u/s}$



Flow-like
pendulum
without
intersections

Preliminary numerical explorations indicates that the probability of capture by the attracting focus can be defined as the **ratio between the entrance/exit strips** (one can avoid homoclinics). Note that this implies $\lim_{\epsilon \rightarrow 0} P_{\text{capture}} > 0$.

To do: IVFs as a numerical tool ok! But theoretical justification is missed!

Thank you for your attention